NANO LETTERS

2007
Vol. 7, No. 3
620−625

Hybrid Structures Composed of Photosynthetic System and Metal Nanoparticles: Plasmon Enhancement Effect

Alexander O. Govorov*,† and Itai Carmeli‡

Department of Physics and Astronomy, Ohio University, Athens, Ohio 45701, and Department of Chemistry, Tel Aviv University, Tel Aviv 69978, Israel

Received October 26, 2006; Revised Manuscript Received January 13, 2007

ABSTRACT

The efficiency of chemical energy production of a photosynthetic system can be strongly enhanced in the presence of metal nanoparticles. Two competing effects contribute to the photosystem efficiency: plasmon enhancement of photon fields inside the light-absorbing chlorophyll molecules and energy transfer from chlorophylls to metal nanoparticles. The first effect can lead to strong enhancement of light absorption by the chlorophylls, whereas the second can somewhat reduce the quantum yield of the system. This paper describes one concrete example of hybrid photosystem that incorporates a photosynthetic reaction center bound to gold and silver nanocrystals. The calculated rate of production of excited electrons inside the reaction center is strongly increased due to plasmon resonance and fast electron–hole separation. In phototransport experiments with photosynthetic reaction centers, the plasma resonance can enhance the photocurrent response. The enhancement mechanism described here can be utilized in energy-conversion devices and sensors.

1. Introduction. Modern nanotechnology opens the possibility of combining solid-state nanocrystals and biomaterials in one superstructure.[1−3] By using bimolecular linkers, one can assemble crystalline nanoparticles, nanowires, and surfaces into complex structures with new physical and chemical properties.[4−6] New properties of a superstructure arise from interactions between building blocks. Such interactions may come from the coupling via electric fields or from charge transfer. One novel type of hybrid structures incorporates photosynthetic molecules and metallic substrates.[7,8] The ongoing experiments with these structures are aimed at the construction of sensitive sensors and efficient photocells and utilize the photosynthetic molecules as an active medium due to their high quantum yield and energy conversion efficiency.

Here we propose and model a novel type of hybrid structures that combines photosynthetic molecular complexes and metal nanoparticles. In our models, we involve two types of nanocrystals, spherical nanoparticles (NPs) and nanoshells (NSs). We show that, due to the plasmon resonances, the chemical production rate in these systems can be greatly enhanced. We should note that the ongoing experiments with photosynthetic molecules and metallic substrates concern photocurrents.[7,8] Since the plasmon effect can increase the generation of electrons inside the photosynthetic complex, such hybrid systems can enhance the performance of devices based on photocurrents in photosynthetic complexes. It should be noted that plasmon-enhanced photocurrents were already observed in recent experiments with metal NPs conjugated to molecules.[9]

2. Model of Hybrid Photosystem. Our model incorporates a photosystem I (PS I) reaction center and a single metal nanocrystal (Figure 1). The PS I reaction center from cyanobacteria (*Synechocystis* sp. PCC6803)[8] is conjugated with a metal nanocrystal through a biolinker. The PS I reaction center is composed of the following elements/cofactors:[10] a chlorophyll dimer (special pair, *P*), two pairs of chlorophylls (eC-B2/ eC-A3 and eC-A2/eC-B3), two quinone molecules ($Q_{A(B)}$), and the iron−sulfur centers (*F*). These building blocks (cofactors) are typical for the reaction centers of many light-harvesting biological systems.[11] Here we assumed that a nanocrystal is attached to the iron-centers side (electron donor side) of the reaction center. In principle, a nanocrystal can be bound to both sides (acceptor or donor). It can be done through a sulfide bond with cysteine mutant in the protein.[8]

Upon absorption of a photon, the special pair *P* is excited to its higher energy singlet state *P**, which transfers an electron along the chains to the chlorophyll cofactors eC −

* Corresponding author. E-mail: govorov@phy.ohiou.edu.
† Ohio University.
‡ Tel Aviv University.

10.1021/nl062528t CCC: $37.00
Published on Web 02/20/2007

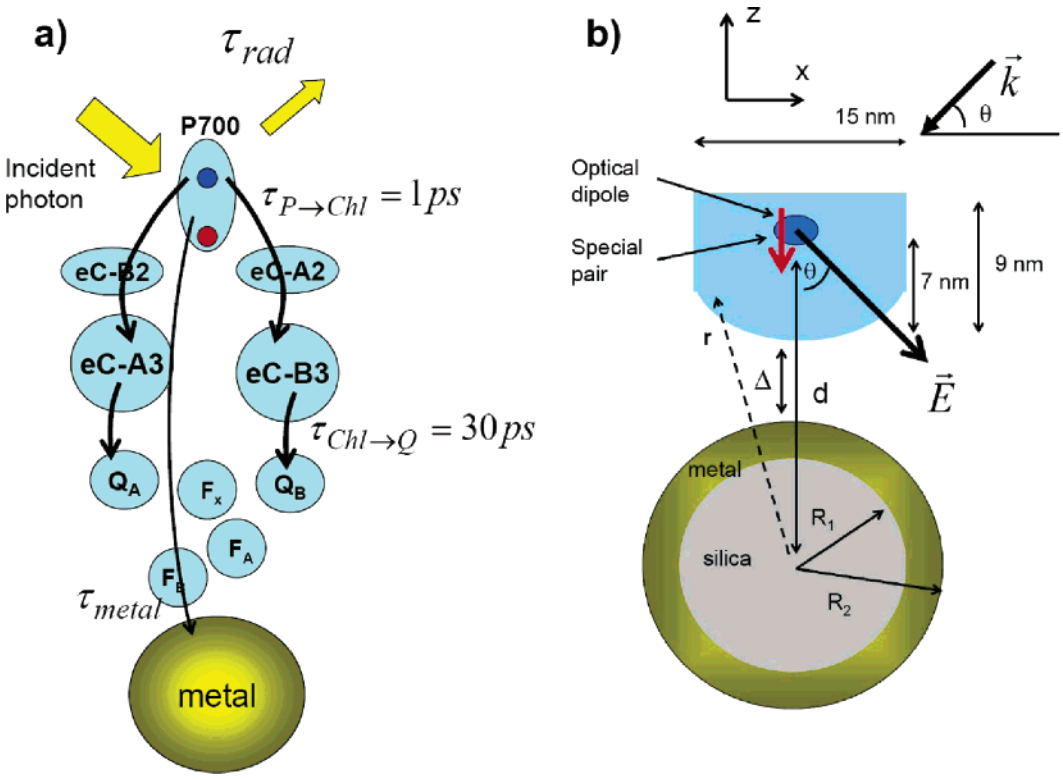

Figure 1. (a) Schematic of the system. (b) Geometry of the system.

A_3/eC − B_3 in about $\tau_{P\to Chl} \approx 1$ ps.[10] The chlorophyll cofactors eC − A_2/eC − B_2 are involved in this initial charge separation process. After fast charge separation, the radiative recombination of the electron−hole pair becomes very unlike. In the next step, the complex P^+eC − B_3^-/P^+eC − A_3^- transfers an electron to the quinone Q_B^-/Q_A^- in about $\tau_{Chl\to Q} = 30$ ps. Here $Q_{A(B)}^-$ denotes a quinone with one extra electron. This final excited state of the system can be noted as $P^+Q_{A(B)}^-$. After the promotion of $Q_{A(B)}$ into its excited state (∼1.2 eV), the quinones transfer electrons to the iron−sulfur clusters in 250 ns to form the excited state P^+/F^-. Since the electron transfer from the special pair to the iron−sulfur clusters is a unidirectional process with almost no losses, we will compute the rate of generation of excited quinones. We should note that whether the two branches are used with similar probability or whether one of them is clearly dominating is presently under discussion.[10] Our derivations will not depend on the number of active branches since we will calculate the total number of excited quinone molecules $Q^- = Q_A^- + Q_B^-$. In the linear regime, the rate equation for the special pair takes a form:

$$\frac{dn_{P*}}{dt} = \alpha \cdot I - \frac{n_{P*}}{\tau_{P\to Chl}} - \frac{n_{P*}}{\tau_{rec}} \qquad (1)$$

where n_{P*} is the average number of excited states of P, $n_{P*} \ll 1$, and α and I are the absorption coefficient and the light intensity at the special pair, respectively. The rate of recombination is $1/\tau_{rec} = 1/\tau_0 + 1/\tau_{metal}$, where τ_0 is the time describing the intrinsic losses from the excited state P^* inside the reaction center and τ_{metal} is the time to transfer of an exciton from P^* to the metal nanocrystal. The time τ_{metal} can become important if the metal NP is located in the very close proximity of P^*. We note that eq 1 describes the unidirectional process from P^* to P^+Q^- since electron transfer occurs with significant reduction of energy (1.8 → 1.2 eV). In the stationary regime, the time derivative in eq 1 is zero and we obtain: $n_{P*} = \alpha \cdot I/\gamma_{tot}$, where $\gamma_{tot} = 1/\tau_{P\to Chl} + 1/\tau_{rec}$. From similar equations for the numbers of excited chlorophylls (P^+eC − B_3^- and P^+eC − A_3^-) and Q^-, we obtain the rate of Q^- generation

$$R_{Q^-} = \frac{n_{P^+Chl^-}}{\tau_{Chl\to Q}} = \frac{\alpha \cdot I}{1 + \tau_{P\to Chl}/\tau_{rec}}$$

where $n_{P^+Chl^-}$ is the number of P^+Chl^- complexes. This equation is valid for the linear regime. The quantum yield of the charge separation process is given by

$$Y = \frac{R_{Q^-}}{\alpha \cdot I} = \frac{1}{1 + \tau_{P\to Chl}/\tau_{rec}} = \frac{1}{1 + \tau_{P\to Chl}/\tau_0 + \tau_{P\to Chl}/\tau_{metal}} \qquad (2)$$

The light intensity $I \propto E^2$, where E is the amplitude of the incident electromagnetic field. In the presence of metal nanocrystal, this amplitude can be strongly changed due to the induced surface charges. The corresponding enhancement factor is defined as

$$P(\omega) = \frac{E_z^2}{E_{z,nometal}^2} \qquad (3)$$

where $E_{z,\text{no metal}}$ is the z-component of the electric field at the P cofactor in the absence of metal nanocrystal and E_z is the amplitude of the actual electric field inside the hybrid PS−metal system. We consider here only the z-components since the optical dipole moment of the reaction center is parallel to the z-axis.[8] Correspondingly, the absorption coefficient strongly depends on the incidence angle: $\alpha = \alpha_0 \cos\theta^2$ (Figure 1b). Then, the rate becomes equal to

$$R_{Q^-} = \frac{\alpha_0 \cdot I_0 \cdot P(\omega) \cdot \cos\theta^2}{1 + \tau_{P\to\text{Chl}}/\tau_0 + \tau_{P\to\text{Chl}}/\tau_{\text{metal}}} \qquad (4)$$

where $I_0 \propto E^2_{\text{nometal}}$.

Our model assumes that the image charges of metal NP do not influence the charge-transfer process within the PS complex. We can justify this approximation by estimating the energy of interaction between the photoexcited electron and the induced dipole moment of a NP. The energy of charge−dipole interaction for the parameters of our model is 0.05−0.1 eV, whereas the reduction of energy of electron during the transfer process is 0.6 eV. Therefore, it is very unlikely that the transfer process will be affected by the electron−NP interaction.

3. Plasmon Effects. Now we focus on calculation of the plasmon enhancement factor $P(\omega)$. The electric potential induced by the incident light in the system shown in Figure 1b has a form:

$$\varphi = -\mathbf{E}_0\mathbf{r} + \beta(\omega)\frac{\mathbf{E}_0\mathbf{r}}{r^3}$$

where $E_{\text{no metal}} = \mathbf{E}_0\, e^{-i\omega t}$ is the laser field and $\mathbf{E}_0$ is its amplitude; r is the radius vector with respect to the center of NP. The function $\beta(\omega)$ describes the induced dipole moment of NP and depends on the NP geometry and dielectric constant. For spherical NP and NS, this function can be calculated from the quasistatic equation $\nabla\epsilon(r)\nabla\varphi = 0$, where $\epsilon(r)$ is the spatially dependent dielectric constant. The coefficients $\beta(\omega)$ for NP and NS are:[12]

$$\beta_{\text{NP}} = R^3\frac{\epsilon_m - \epsilon_0}{(2\epsilon_0 + \epsilon_m)},$$

$$\beta_{\text{NS}} = \frac{R_2^3[R_1^3(\epsilon_d - \epsilon_m)(\epsilon_0 + 2\epsilon_m) - R_2^3(\epsilon_0 - \epsilon_m)(\epsilon_d + 2\epsilon_m)]}{[2R_1^3(\epsilon_0 - \epsilon_m)(-\epsilon_d + \epsilon_m) + R_2^3(2\epsilon_0 + \epsilon_m)(\epsilon_d + 2\epsilon_m)]}$$

here R is the NP radius, $R_{1(2)}$ are the inner and outer radii of NS, respectively. The parameters ϵ_0, ϵ_m, and ϵ_d denote the dielectric constants of matrix, metal, and dielectric core of NS, respectively. The resultant electric field is given by $\vec{E} = \vec{E}_0 + [3(\vec{a}\cdot\vec{n})\vec{n} - \vec{a}]/r^3$, where $\vec{a} = \beta\vec{E}_0$. Then the enhancement factor takes the form:

$$P(\omega) = |1 + \frac{2\beta}{d^3}|^2 \qquad (5)$$

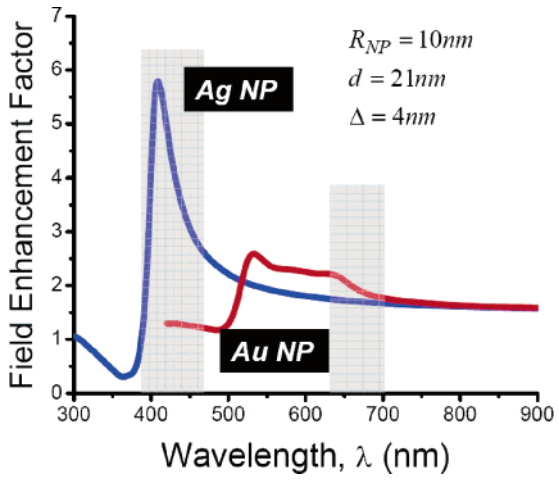

Figure 2. Calculated enhancement factors for Au and Ag NPs as a function of the wavelength.

Figures 2 and 3 show calculated enhancement factors for our geometry. In our calculations, we use $\epsilon_0 = \epsilon_d = 2.2$; this value for ϵ_d corresponds to the dielectric constant of silica. We also take the matrix dielectric constant ϵ_0 slightly increased from the water value ($\epsilon_w = 1.8$) to account for the presence of biological molecules. The condition for the plasmon enhancement inside the system is the following:

$$\hbar\omega_{\text{abs}} \approx \hbar\omega_{\text{plasmon peak}}$$

where $\hbar\omega_{\text{plasmon peak}}$ and $\hbar\omega_{\text{abs}}$ are the plasmon peak position of NP/NS and the absorption peak position of PS system, respectively. The PS reaction center studied in ref 8 has maxima in the absorption spectrum at $\hbar\omega_{\text{abs}} \approx 1.83$ and 2.83 eV ($\lambda \approx 673$ and 436 nm). Grey zones in Figures 2 and 3 correspond to the wavevector intervals where this particular reaction center[8] absorbs photons. Other bacterial and plant systems have somewhat similar regions of absorption of sun radiation. We see from Figures 2 and 3 that significant enhancement can be achieved for a silver NP at about 436 nm and for both gold and silver nanoshells at about 673 nm.

The calculated plasmon resonances in single Au and Ag spherical nanocrystals (i.e., NPs) lie at about 530 and 420 nm, correspondingly. Since the absorption wavelengths of PS I reaction center are at approximately 436 and 673 nm, the Au NPs are not suitable for the plasmon enhancement effect. However, single Ag NPs can be used. Recently, it was suggested that nanoshells (NSs) can be successfully used to shift plasmon resonances to the red.[13] In addition to the plasmon shift effect, we see for a NS a stronger enhancement effect compared to that of a NP (compare Figures 2 and 3). The maximum enhancement factors for an Ag NP (at about 420 nm), Ag NS (at about 670 nm), and Au NS (680 nm) are the following 6, 15, 10, correspondingly. Especially, Ag NSs demonstrate remarkable enhancement for $P(\omega)$ and for the corresponding photon-absorption rate $\alpha_0\cdot I_0\cdot P(\omega)$. The strongest enhancement can be achieved by using Ag nanocrystals since Ag has stronger plasmon resonances. This was also noticed in refs 4, 14. From first look, one can expect appearance of splitting in the plasmon spectrum $P(\omega)$ due

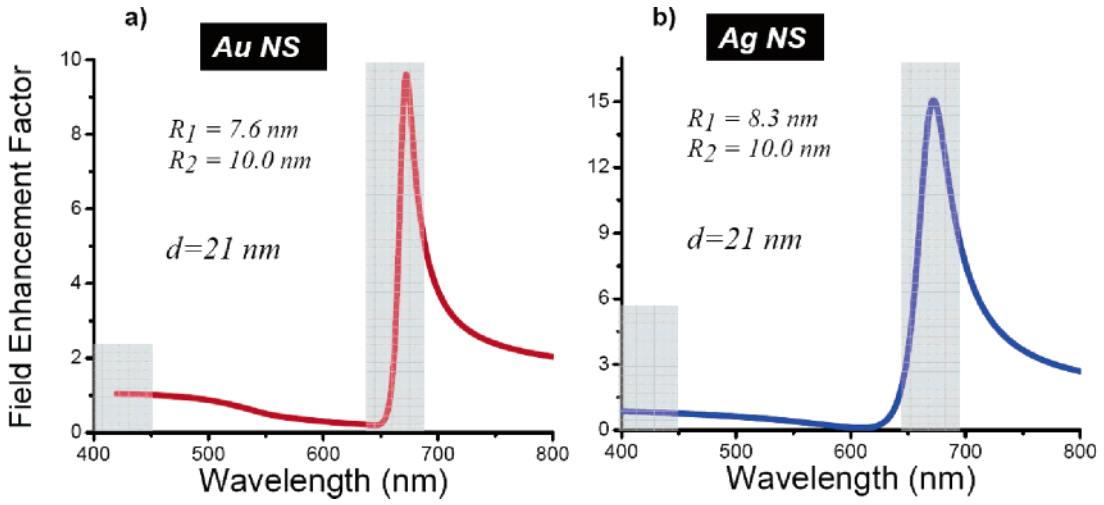

Figure 3. Calculated enhancement factors for Au and Ag nanoshells as a function of the wavelength.

to the interaction between two plasmons localized near the inner and outer surfaces of the NS.[13] However, we do not see this splitting. The reason is that we use empirical dielectrics functions for Au and Ag, which give strong broadening to plasmon resonances and also include interband transitions. It is easy to see that, for the Drude dielectric function with a small plasmon broadening, the function $P(\omega)$ clearly demonstrates the splitting of the plasmon peak.

The enhancement factor was calculated above for the z-component of the electric field because the absorbing dipole moment is assumed to be in the z-direction. For our geometry (Figure 1b), it means that the dipole moment is perpendicular to the surface of nanocrystal. This configuration is most advantageous for the plasmon enhancement effect.[15] For example, if the optical dipole is parallel to the nanocrystal surface, the factor $P(\omega)$ can be either suppressed (NP) or slightly enhanced (NS). For estimations, one can use the equation:

$$P_x(\omega) = \frac{E_x^2}{E_{x,\text{nometal}}^2} = |1 - \frac{\beta}{d^3}|^2$$

Now we discuss the effect of metal NPs/NS on the quantum yield of quinone production. To calculate this, we use the fluctuation−dissipation theorem and the method developed in ref 15. The energy transfer time for a dipole is given by $1/\tau_{\text{metal}}(\omega) = -2/\hbar\ \text{Im}\ F(\omega)$, where $F(\omega)$ is the response function. In the dipole limit ($d > R_{\text{NP}}, R_2$), we can obtain analytical results (for details see ref 15)

$$\frac{1}{\tau_{\text{metal,NP/NS}}(\omega)} = -\frac{8}{\hbar}\frac{e^2 \cdot d_{\text{sp}}^2}{d_6\,\epsilon_0^2}\frac{\text{Im}[\epsilon_m(\omega)]}{4\pi} f_{\text{NP/NS}}(\omega),$$

$$f_{\text{NP}}(\omega) = \frac{4\pi}{3}R_{\text{NP}}^3\left|\frac{3\epsilon_0}{\epsilon_m(\omega) + 2\epsilon_0}\right|^2 \quad (6)$$

For the NS case, the function $f_{\text{NS}}(\omega)$ is rather complex and is given in the Supporting Information. Equation 6 describes the energy transfer from a z-oriented dipole. The transfer times depend on the dipole moment of the special pair d_{sp}. To estimate this parameter, we use the expression for a molecular radiative lifetime[16] $1/\tau_{\text{rad}} = 8\pi\sqrt{\epsilon_0}\omega_{\text{exc}}^3\ e^2 d_{\text{sp}}^2/3h{\cdot}c^3$, where $\hbar\omega_{\text{exc}}$ is the exciton energy of the special pair. With typical molecular radiative lifetime $\tau_{\text{rad}} \approx 5$ ns and $\hbar\omega_{\text{exc}} \approx 1.8$ eV, we obtain $d_{\text{sp}} \approx 0.26$ nm. The above value is a typical number for molecular systems. First we calculate the transfer times for Au and Ag nanoshells. In the absence of the metal subsystem, the quantum yield is close to unit. Taking $\tau_{\text{rad}} \approx 5$ ns and $\tau_{P\to\text{BPh}} = 4$ ps, we have $Y_0 \approx 0.999$. Figure 4 shows the transfer times τ_{metal}, quantum yield Y, and the relative quinone production rates:

$$\frac{R_{Q^-}}{R_{Q^-}^0} = P(\omega)\frac{Y}{Y^0} = P(\omega)\frac{1 + \tau_{P\to\text{Chl}}/\tau_0}{1 + \tau_{P\to\text{Chl}}/\tau_0 + \tau_{P\to\text{Chl}}/\tau_{\text{metal}}}$$

Here $R_{Q^-}^0$ and Y_0 are the corresponding values in the absence of the metal subsystem. In Figure 4, we see a remarkable enhancement of the production rate $R_{Q^-}/R_{Q^-}^0$. As it was expected, the quantum yield of the PS reaction center becomes reduced due to the energy transfer to the metal. However, this decrease is significantly less than the field enhancement $P(\omega)$. Both quantities, $Y(\omega)$ and $P(\omega)$, become strongly changed in the vicinity of the plasmon resonance. The minimum of $Y(\omega)$ is slightly to the blue compared to the maximum of $P(\omega)$. This behavior makes the enhancement effect even stronger.

Equations 2 and 4 describing the plasmon effects have two important parameters: enhancement factor $P(\omega)$ and energy dissipation rate $1/\tau_{\text{metal}}$. The net effect on the production rate depends on competition between the above parameters. The same interplay of field enhancement and energy dissipation was found for the emission process of semiconductor NPs in the vicinity of the metal nanocrystals.[4,15] The parameters $P(\omega)$ and $1/\tau_{\text{metal}}$ strongly depend on the geometry, dipole orientation, and nanocrystal material. Therefore, the design of hybrid structures and the understanding of physical mechanisms can be crucial.

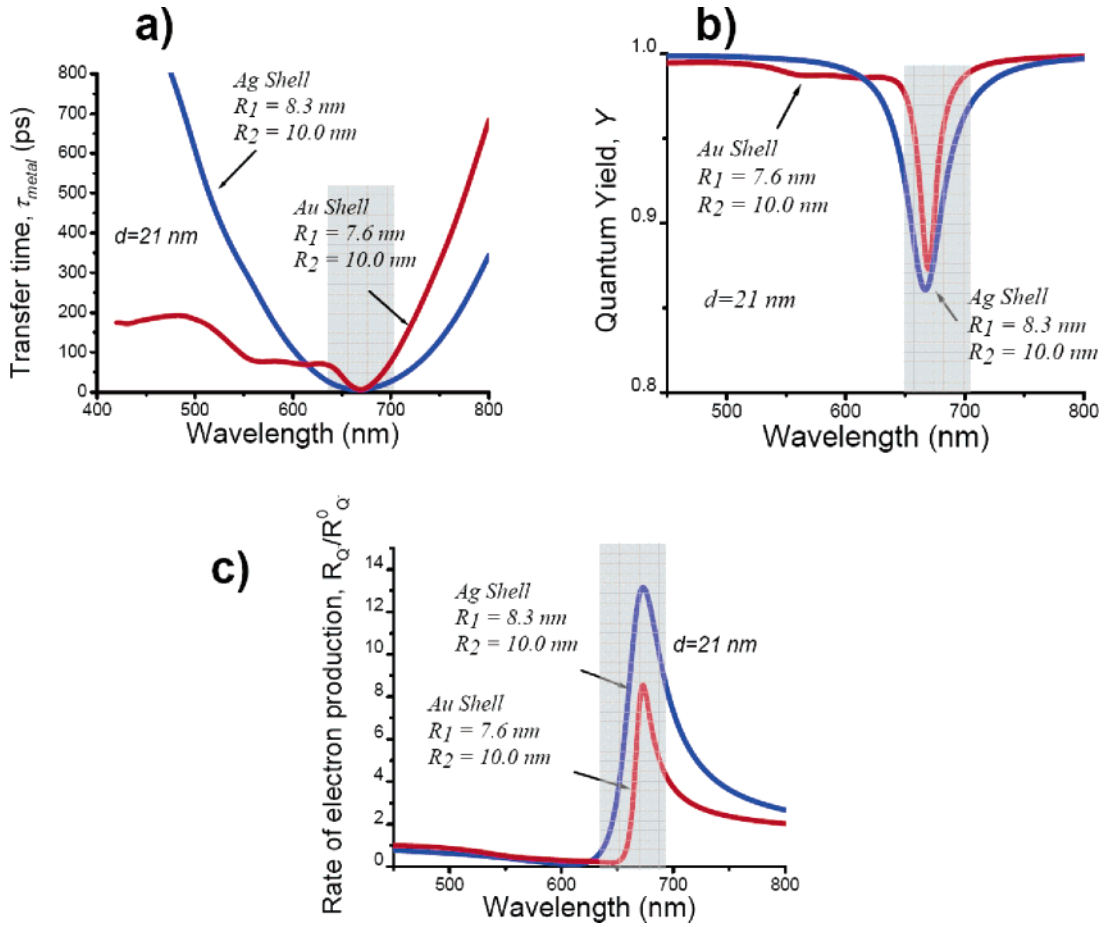

Figure 4. (a) Calculated enhancement energy transfer time for Au and Ag nanoshells; (b) and (c) quantum yield and relative rate of quinone production for the same hybrids.

In the case of Ag NP, the plasmon enhancement effect is expected at about 430 nm (Figure 2). In this case, the exciton in the special pair is created indirectly. First, the photon creates the excitation with energy 2.83 eV ($\lambda \approx 436$ nm). Then, the system makes transition to the state with energy 1.83 eV ($\lambda \approx 673$ nm). Using the rate equation, we obtain the quantum yield $Y(\omega) \approx 1 - (\tau_{\text{exc}\rightarrow P^*}/\tau_{0,\text{exc}} + \tau_{\text{exc}\rightarrow P^*}/\tau_{\text{metal,2.83eV}}(\omega) + \tau_{P\rightarrow\text{Chl}}/\tau_{0,P^*} + \tau_{P\rightarrow\text{Chl}}/\tau_{\text{metal,1.83eV}})$, where $\tau_{\text{metal,1.83eV}}$ is the PS−metal transfer time at the specified energy and $\tau_{\text{exc}\rightarrow P^*}$ is the relaxation time from the exciton to the state P^* with the exciton energy of 1.83 eV. For the time $\tau_{\text{exc}\rightarrow P^*}$, we took 2 ps. The above simplified equation is valid if the transfer times $\tau_{\text{metal}} \gg \tau_{P\rightarrow\text{Chl}}, \tau_{\text{exc}\rightarrow P^*}$. Figure 5 summarizes the results for the Ag NP. Again we observe significant enhancement of the normalized quinone production rate $R_{Q^-}/R^0_{Q^-}$. We also note that the energy transfer times in the regime of small d ($d \approx R,R_{1(2)}$) should be calculated numerically. One convenient numerical method is described in ref 15; it incorporates the multipole expansion approach and fluctuation−dissipation theorem.

4. Discussion. An advantage of the proposed hybrid system is that more chemical energy (number of excited electrons) can be produced with a smaller number of reaction centers. The same holds for the case of photocurrent created by a monolayer of reaction centers assembled in the recent experiment.[7,8] The enhancement factors for the nanocrystals

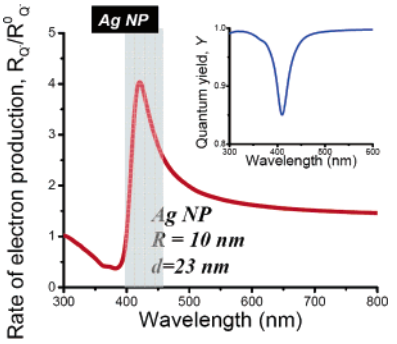

Figure 5. Calculated rate of quinone production for a single Ag NP conjugated with a reaction center. Inset: quantum yield for the same system.

modeled here are about 5−15. If we choose larger metal nanocrystals or design a special nanocrystal complex,[4,15] the enhancement factor of electron production $R_{Q^-}/R^0_{Q^-}$ can be further increased. The PS−nanocrystal complexes can be studied in solution (a), as a monolayer bound to a metal surface (b), and inside biological membranes (c). In the case (a), one can study the effect of plasmon-enhanced absorption by a photosynthetic complex. In the case (b), a monolayer of hybrids can be placed between conducting surfaces and photocurrent can be studied. In nature, bacterial and other reaction centers are built in a membrane and surrounded by

the antenna chlorophylls. These chlorophylls absorb photons and transfer optically created excitons toward the reaction center. With metal nanocrystals, one can also enhance optical absorption of the antenna chlorophylls. For efficient light harvesting, the Förster transfer times[17] should be smaller than the time of transfer to metal. Also, the Förster transfer process itself can be affected by the metal nanocrystals, and the whole problem becomes more complex and needs special treatment.[18]

Enhanced generation of excited electrons appear due to increased absorption and very fast change separation within a photosynthetic molecule. The photogenerated electron and hole become spatially separated very fast, within about 1 ps. This time is shorter than the time to transfer exciton energy to a metal nanocrystal. This inequality ($\tau_{P\rightarrow Chl} \ll \tau_{metal}$) insures that the energy losses are relatively small. Finally, we note that a photosynthetic system with fast spatial charge separation somewhat resembles photodiodes and type-II semiconductor heterostructures in which photogenerated electron−hole pairs became rapidly separated in space due to the built-in potential.[19] Compared to solid-state devices, advantages of hybrid systems are in three-dimensional architecture and self-assembly and in photochemical responses.

5. Conclusions. To summarize, we proposed and modeled a hybrid system composed of photosynthetic molecules and metal nanoparticles and nanoshells. Despite a reduced quantum yield, plasmon resonances in such a system can greatly enhance photochemical production or photocurrents.

Acknowledgment. We thank F. Simmel (Munich University) and C. Carmeli (Tel Aviv University) for very helpful discussions. This work was supported by NSF and BioNanoTechnology Initiative at Ohio University.

Supporting Information Available: The function equation $f_{NS}(\omega)$ for the NS case. This material is available free of charge via the Internet at http://pubs.acs.org.

References

(1) Cui, Y.; Wei, Q.; Park, H.; Lieber, C. M. *Science* **2001**, *293*, 1289.
(2) Alivisatos, A. P.; Johnsson, K. P.; Peng, X.; Wilson, T. E.; Loweth, C. J.; Bruchez, M. P., Jr.; Schultz, P. G. *Nature* **1996**, *382*, 609.
(3) Mirkin, C. A.; Letsinger, R. L.; Mucic, R. C.; Storhoff, J. J. *Nature* **1996**, *382*, 607.
(4) Lee, J.; Govorov, A. O.; Kotov, N. A. *Angew. Chem.* **2005**, *117*, 7605. Lee, J.; Govorov; A. O.; Dulka, J.; Kotov, N. A. *Nano Lett.* **2004**, *4*, 2323.
(5) Slocik, J. M.; Govorov, A. O.; Naik, R. R. *Supramol. Chem.* **2006**, *18*, 415.
(6) Liedl, T.; Olapinski, M.; Simmel, F. C. *Angew. Chem.* **2006**, *45*, 5007.
(7) Das, R.; Kiley, P. J.; Segal, M.; Norville, J.; Yu, A. A.; Wang, L.; Trammell, A. S.; Reddick, L. E.; Kumar, R.; Stellacci, F.; Lebedev, N.; Schnur, J.; Bruce, B. D.; Zhang, S.; Baldo, M. *Nano Lett.* **2004**, *4*, 1079.
(8) Frolov, L.; Rosenwaks, Y.; Carmeli, C.; Carmeli, I. *Adv. Mater.* **2005**, *17*, 2434.
(9) Akiyama, T.; Nakada, M.; Terasaki, N.; Yamada, S. *Chem. Commun.* **2006**, 4, 395; Ishida, A.; T. Majima, T. *Chem. Phys. Lett.* **2000**, *322*, 242; Fukuda, N.; Mitsuishi, M.; Aoki, A.; Miyashita, T. *Chem. Lett.* **2001**, 378.
(10) Brettel, K.; Leibl, W. *Biochim. Biophys. Acta* **2001**, *1507*, 100.
(11) Kirmaier, C.; Weems, D.; Holten, D. *Biochemistry* **1999**, *38*, 11516.
(12) Landau, L. D.; Lifshitz, E. M. *Electrodynamics of Continuous Media*; Pergamon: New York, 1960.
(13) Halas, N. *MRS Bull.* **2005**, *30*, 362.
(14) Jiang Jiang, Bosnick, K.; Maillard, M.; Brus, L. *J. Phys. Chem. B* **2003**, *107*, 9964.
(15) Govorov, A. O.; Bryant, G. W.; Zhang, W.; Skeini, T.; Lee, J.; Kotov, N. A.; Slocik, J. M.; Naik, R. R. *Nano Lett.* **2006**, *6*, 984.
(16) Yariv, A. *Quantum Electronics*, 2nd ed.; John Wiley & Sons: New York, 1975.
(17) Hu, X.; Damjanovic, A.; Ritz, T.; Schulten, K. *Proc. Natl. Acad. Sci. U.S.A.* **1998**, *95*, 5935.
(18) Govorov, A.O.; Lee, J.; Kotov, N. A. Unpublished.
(19) Sze, S. M. *Physics of Semiconductor Devices*, John Wiley & Sons: New York, 1982.

NL062528T